Human thiopurine *S*-methyltransferase pharmacogenetics: Variant allozyme misfolding and aggresome formation

Liewei Wang[†], Tien V. Nguyen[†], Richard W. McLaughlin[‡], Laura A. Sikkink[‡], Marina Ramirez-Alvarado[‡], and Richard M. Weinshilboum[†§]

Departments of [†]Molecular Pharmacology and Experimental Therapeutics and [‡]Biochemistry and Molecular Biology, Mayo Clinic College of Medicine, Rochester, MN 55905

Communicated by Allan H. Conney, Rutgers, The State University of New Jersey, Piscataway, NJ, March 22, 2005 (received for review February 2, 2005)

Thiopurine *S*-methyltransferase (TPMT) catalyzes the S-methylation of thiopurine drugs. TPMT genetic polymorphisms represent a striking example of the potential clinical value of pharmacogenetics. Subjects homozygous for *TPMT*3A*, the most common variant allele for low activity, an allele that encodes a protein with two changes in amino acid sequence, are at greatly increased risk for life-threatening toxicity when treated with standard doses of thiopurines. These subjects have virtually undetectable levels of TPMT protein. In this study, we tested the hypothesis that *TPMT*3A* might result in protein misfolding and aggregation. We observed that TPMT*3A forms aggresomes in cultured cells and that it aggregates *in vitro*, functional mechanisms not previously described in pharmacogenetics. Furthermore, there was a correlation among TPMT half-life values in rabbit reticulocyte lysate, aggresome formation in COS-1 cells, and protein aggregation *in vitro* for the three variant allozymes encoded by alleles that include the two *TPMT*3A* single-nucleotide polymorphisms. These observations were compatible with a common structural explanation for all of these effects, a conclusion supported by size-exclusion chromatography and CD spectroscopy. The results of these experiments provide insight into a unique pharmacogenetic mechanism by which common polymorphisms affect TPMT protein function and, as a result, therapeutic response to thiopurine drugs.

thiopurine toxicity | protein aggregation | pharmacogenomics | protein degradation

Pharmacogenetics is the study of the role of inheritance in individual variation in response to drugs (1). The clinical goals of pharmacogenetics are to avoid adverse drug reactions, to maximize drug efficacy, and to select patients responsive to a particular therapeutic agent or class of agents. When a drug is administrated orally, it is absorbed and distributed, interacts with its targets, is metabolized, and finally is excreted. Potentially, pharmacogenetics has implications for each of these steps. However, drug-metabolizing enzymes have been studied most intensively from a pharmacogenetic perspective, and thiopurine *S*-methyltransferase (TPMT) is one of the most striking examples of the clinical relevance of genetic variation in drug metabolism (1).

TPMT is a cytosolic drug-metabolizing enzyme that catalyzes the S-methylation of thiopurine drugs such as 6-mecaptopurine and azathioprine (2–4). Thiopurine drugs are used to treat childhood leukemia, autoimmune diseases, and transplant recipients (2–4). However, these agents have a narrow therapeutic index with potentially life-threatening drug-induced toxicity (4–6). Large individual variations in levels of TPMT activity in human tissues are regulated primarily by common genetic polymorphisms (7–10). *TPMT*3A*, the most common variant allele in Caucasians (5% frequency), has two nonsynonymous coding SNPs, whereas *TPMT*3C*, the most common variant allele in East Asia (2% frequency), includes only the codon 240 SNP, and the rare *TPMT*3B* allele has only the codon 154 SNP (Fig. 1*A*) (10–12). The presence of *TPMT*3A* results in virtual lack of TPMT protein and, as a result, enzyme activity (10). Patients homozygous for *TPMT*3A* can suffer severe, life-threatening toxicity when treated with standard doses of thiopurines (6, 13). Therefore, to avoid toxicity, these patients must be treated with from 1/10th to 1/15th of the standard dose (11, 12, 14). Because of its clinical importance, the Food and Drug Administration listed TPMT as one of only two "valid biomarkers" for pharmacogenomics in its 2003 "Draft Guidance for Pharmacogenomic Data Submission" (15).

Because TPMT represents one of the most striking and frequently cited examples of the clinical significance of pharmacogenetics (12), it is important to understand mechanisms by which the common polymorphisms in *TPMT*3A* influence protein function. Previous studies showed that the presence of *TPMT*3A* results in virtually no enzyme activity or protein, both in human tissues and after transient expression in COS-1 cells (10, 16). The decreased level of enzyme protein was due to rapid degradation by a ubiquitin (Ub)/proteasome-dependent process, with the involvement of chaperone proteins (16, 17). Those observations suggested that TPMT*3A might be misfolded and targeted for degradation by the protein quality control process (18). That process results in a dynamic balance among proper folding, degradation, and aggregation (19). The recent description of the aggresome has served to clarify one mechanism by which misfolded proteins are handled in the cell (20–22). Aggresomes are pericentriolar cytoplasmic structures in which aggregated, multiubquitinated misfolded proteins are sequestered (20).

The fact that the two common polymorphisms in the *TPMT* gene (Fig. 1*A*) result in rapid protein degradation, and that molecular chaperones are involved in this process, led us to test the hypothesis that these two polymorphisms might result in protein misfolding and, possibly, aggregation. In the present study, we have demonstrated that the TPMT *3A, *3B, and *3C allozymes all form typical aggresomes in COS-1 cells, with a rank order that correlates with rates of allozyme degradation in a rabbit reticulocyte lysate (RRL) and with the *in vitro* aggregation of *Escherichia coli* recombinant allozymes. Furthermore, the application of size-exclusion chromatography and CD spectroscopy supports the presence of structural differences between WT and variant TPMT allozyme monomers and aggregates.

Materials and Methods

COS-1 Cell Expression. N-terminal hemagglutinin (HA)-tagged WT, *3A, *3B, and *3C TPMT constructs were created and cloned into the eukaryotic expression vector pCR3.1 (Invitrogen). COS-1 cells were transfected with equal quantities of

Freely available online through the PNAS open access option.

Abbreviations: TPMT, thiopurine *S*-methyltransferase; RRL, rabbit reticulocyte lysate; Ub, ubiquitin; IP, immunoprecipitation; HDAC, histone deacetylase; HA, hemagglutinin.

[§]To whom correspondence should be addressed. E-mail: weinshilboum.richard@mayo.edu.

www.pnas.org/cgi/doi/10.1073/pnas.0502352102

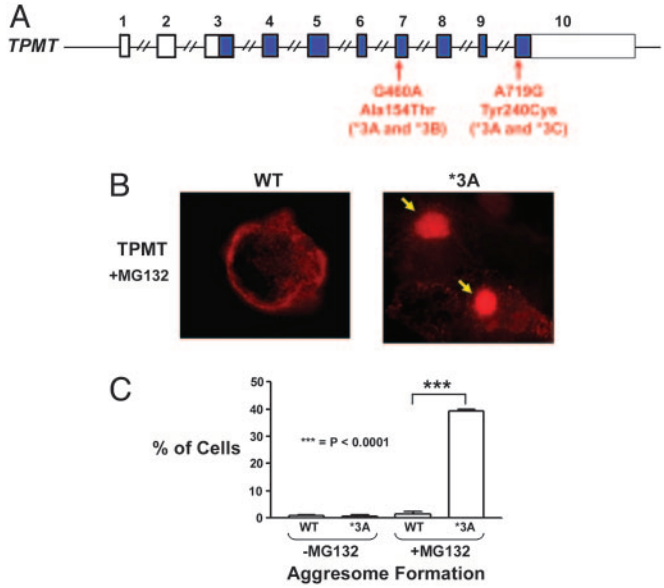

Fig. 1. *TPMT* gene structure and aggresome formation. (*A*) *TPMT*3A* contains two SNPs, **3B* contains only the G460A SNP, and **3C* contains only the A719G SNP. (*B*) TPMT*3A aggresome formation. COS-1 cells were transiently transfected with HA-tagged WT and *3A TPMT constructs, treated with MG132, and then subjected to fluorescence microscopy. Yellow arrows point to aggresomes. (*C*) Aggresome formation after the transfection of COS-1 cells with WT or *3A TPMT represented as the percentage of ≈200 cells counted (mean ± SEM, $n = 4$).

pCR3.1 expression construct DNA by using the TransFast transfection reagent (Promega). In some experiments, cells were cotransfected with a Myc-tagged Ub construct. The cells were then treated for 20 h with either DMSO or 20 μM MG132 (a proteasome inhibitor) dissolved in DMSO, followed by harvest in 0.1% Nonidet P-40 lysis buffer. After centrifugation at 14,000 × *g* for 10 min, cell supernatants were used to perform either immunoblotting or immunoprecipitation (IP) studies. In some experiments, cell pellets also were isolated and dissolved in lysis buffer, followed by sonication at 4°C. The sonicated pellets were then centrifuged at 14,000 × *g*, and supernatants from that step were used for immunoblot or IP analysis.

IP and Immunoblot Analysis. Cytosol or pellets from cells cotransfected with Myc-tagged Ub and WT or *3A HA-tagged TPMT constructs were used to perform IP. Specifically, polyclonal anti-HA antibody (Upstate, Charlottesville, VA) was incubated overnight with protein A Sepharose beads (Sigma), followed by incubation for 2 h with cytosol or pellet preparations. The beads were then washed four times with lysis buffer, and bound proteins were dissolved in SDS sample buffer. These mixtures were subjected to 10% SDS/PAGE, and the proteins were transferred to poly(vinylidene difluoride) membranes, followed by blotting with monoclonal anti-HA, polyclonal anti-Myc, or monoclonal anti-Ub antibodies (Sigma).

Immunofluorescence Microscopy. COS-1 cells were transfected with HA-tagged WT, *3A, *3B, or *3C TPMT constructs, followed by treatment for 20 h with 20 μM MG132. In some experiments, the cells were treated with 1 μM vinblastine (Sigma) or with 10 μM scriptaid (Alexis Biochemicals, San Diego), a histone deacetylase (HDAC) inhibitor, for 4 h before the addition of MG132. Immunofluorescence microscopy of aggresome components was performed as described in ref. 41. To study HDAC6, the cells were incubated with monoclonal anti-HA antibody, 1:200, and polyclonal anti-HDAC6, 1:25, (BioVision, Mountain View, CA), followed by secondary antibody. Approximately 200 cells were counted for aggresomes in each of four randomly selected regions.

***In Vitro* Translation and Degradation.** [^{35}S]Methionine-labeled, *in vitro* translated WT, *3A, *3B, and *3C TPMT were generated with the TNT RRL *in vitro* translation system (Promega), and these proteins were used to perform degradation studies as described in ref. 16.

Bacterial Recombinant TPMT. Human WT, *3A, *3B, and *3C TPMT constructs in the bacterial expression vector pGEX6P2 were transformed into BL21 *E. coli* to express TPMT–GST fusion proteins. Purification of the recombinant TPMT–GST fusion proteins and cleavage of the GST tag were performed at 4°C. The recombinant proteins were then separated and purified by size-exclusion chromatography on an FPLC (Amersham Pharmacia Biosciences) by using a 16 mm × 60 cm gel filtration column (Superdex 75, Amersham Pharmacia Biosciences) with 20 mM potassium phosphate buffer, pH 7.3, containing 2% glycerol. The purity of recombinant TPMT allozyme fractions after chromatography was determined by SDS/PAGE and immunoblot analysis. TPMT activity also was measured in the FPLC chromatography fractions by using the radiochemical assay described by Weinshilboum *et al.* (24). The same assay was used to perform substrate kinetic studies with WT and *3C TPMT monomer fractions.

CD Spectroscopy. CD spectra were recorded on an AVIV 215 spectrometer (Proterion, Somerset, NJ). Protein secondary structure measurements were performed by obtaining far-UV CD spectra (260–200 nm) in the continuous mode, taking measurements every 1 nm with an averaging time of 5 sec at 4°C and with a 1-cm pathlength cuvette. Protein concentrations were ≈2 μM. Ellipticity of maximum β-sheet signal also was monitored every 2°C, from 4°C to 90°C, with an equilibration time of 1 min between each temperature point and an averaging time of 60 sec. Thermal denaturation curves were analyzed according to a two-state transition model. Linear extrapolation of the folded and the unfolded baselines was performed by using a minimum of 10 points. Ellipticities of the folded and unfolded states were derived from the extrapolated baselines.

Transmission EM. A 3-μl aliquot of ≈4 μM WT or *3A TPMT was placed on a 300-mesh copper grid. Samples were stained with 4% uranyl acetate and were examined by transmission EM (1200 EX, JEOL).

Statistical Analysis. Differences between groups were determined by using Student's *t* test with the PRISM program (GraphPad, San Diego).

Results

TPMT*3A Aggresome Formation. Misfolded proteins often are targeted for degradation, but when the protein degradation capacity is exceeded, they also may accumulate in aggresomes (19, 21, 22). However, there is no evidence that common nonsynonymous coding SNPs in genes encoding drug-metabolizing enzymes of pharmacogenetic significance can result in aggresome formation. To test that possibility, we performed immunofluorescence with COS-1 cells transiently transfected with HA-tagged WT and *3A TPMT expression constructs. Aggresome formation was observed in ≈40% of COS-1 cells transfected with TPMT*3A after 20 h of treatment with the proteasome inhibitor MG132, compared with <1% of cells transfected with WT TPMT (Fig. 1 *B* and *C*). Aggresomes are detergent-insoluble, so we also prepared immunoblots to determine the possible redistribution of TPMT*3A from cytosol

PHARMACOLOGY

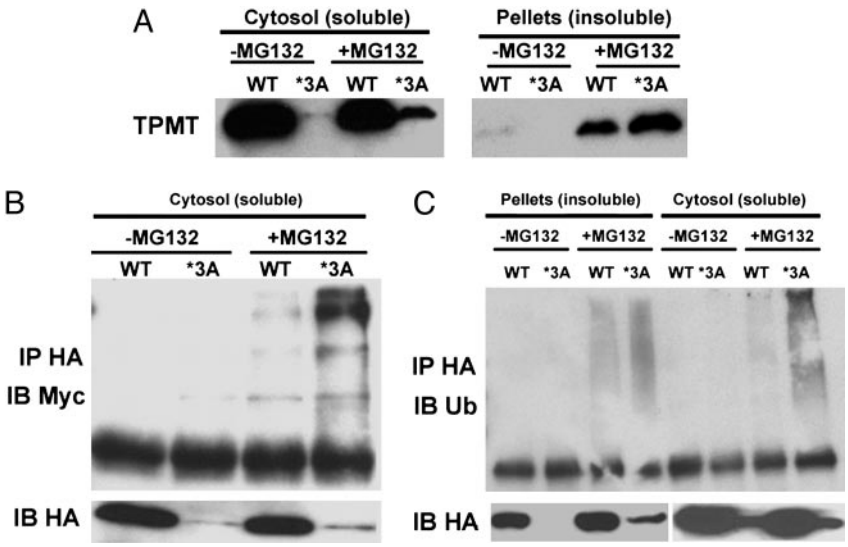

Fig. 2. TPMT redistribution after proteasome inhibition. (*A*) COS-1 cells were transfected with WT or *3A HA-tagged constructs and were treated with either DMSO or MG132. Immunoblot analysis was then performed with an anti-HA antibody. (*B*) TPMT polyubiquitination. HA-tagged WT or *3A TPMT was cotransfected into COS-1 cells with Myc-tagged Ub. The cells were treated with DMSO or MG132, and IP was performed with anti-HA antibody, followed by immunoblot analysis with anti-Myc or anti-HA antibodies. (*C*) Polyubiquitination of redistributed TPMT*3A. HA-tagged WT or *3A and Myc-tagged Ub were transiently expressed in COS-1 cells. IP was then performed with either supernatant from cytosol or resuspended cell pellets, and ubiquitinated TPMT was detected with an anti-Ub antibody.

to pellet, the subcellular fraction that contains aggresomes, after proteasome inhibition. After treatment with MG132, there was the anticipated increase in cytosolic *3A (Fig. 2*A*). However, levels of both WT and *3A TPMT increased to an even greater degree in the cell pellets after MG132 exposure, although, proportionally, there was a larger increase for *3A (Fig. 2*A*).

TPMT*3A Ubiquitination. Previous studies in the RRL demonstrated that TPMT*3A is highly ubiquitinated and targeted for proteasome-mediated degradation (16, 17). To determine the possible role of Ub in the cell as opposed to the RRL, we performed IP with COS-1 cell lysates after the overexpression of WT and *3A TPMT as well as Myc-tagged Ub. The results confirmed that, in the presence of MG132, TPMT*3A also was highly ubiquitinated in the COS-1 cells, even though much less *3A protein was immunoprecipitated than was WT (Fig. 2*B*). It has been reported that genetically variant proteins can be ubiquitinated in the aggresome (20). Therefore, we next asked whether TPMT*3A in the cell pellets, presumably in aggresomes, also was polyubiquitinated. To answer that question, IP was performed with preparations from both cytosol and detergent-insoluble pellets from transfected COS-1 cells. Polyubiquitinated protein was increased to a greater extent for *3A than for WT in the presence of MG132, in both cytosol and pellets, even though less *3A was immunoprecipitated (Fig. 2*C*). The fact that TPMT*3A was ubiquitinated in aggresomes raises the possibility that, even in the aggresome, the variant allozyme might be targeted for proteasome-mediated degradation.

TPMT*3A Aggresome Components. We next determined whether TPMT*3A-positive aggresomes had typical structural features (20, 25, 26), To do that, fluorescence microscopy was performed with polyclonal anti-HA antibody to detect TPMT and with monoclonal antibodies for a series of known aggresome components (Fig. 3). WT TPMT staining was distributed throughout the cytosol, but TPMT*3A staining was localized to aggresomes and colocalized with typical aggresome components. Aggresome formation is microtubule-dependent, with the involvement of dynein. Dynein colocalized to TPMT*3A aggresomes (Fig. 3*B*) as did γ-tubulin, a marker for the centrosome/microtubule organizing center (27) (Fig. 3*C*). In addition, both Ub and molecular chaperones have been shown to interact with aggregation-prone proteins and to contribute to their re-folding and/or degradation (25, 28), and both hsp70 and hsp90 are highly associated with TPMT*3A in the RRL (16). Therefore, it was not surprising that we observed the colocalization of hsp70, hsp90, and Ub with *3A in aggresomes (Fig. 3 *D–F*).

TPMT*3A Aggresomes, Microtubules, and HDAC6. Aggresome formation is microtubule-dependent (20, 26, 29). To study the functional involvement of microtubules in TPMT*3A aggresome formation, cells transfected with WT and *3A TPMT in the presence of MG312 were treated with the microtubule destabilizing agent vinblastine. Vinblastine had no visible effect on cells transfected with WT TPMT. However, it significantly decreased *3A aggresome formation (Fig. 4*A*) but without the disruption of TPMT*3A microaggregates (Fig. 4*D*). These data suggested that intact microtubules are required for the formation of TPMT*3A-containing aggresomes, probably as a result of the

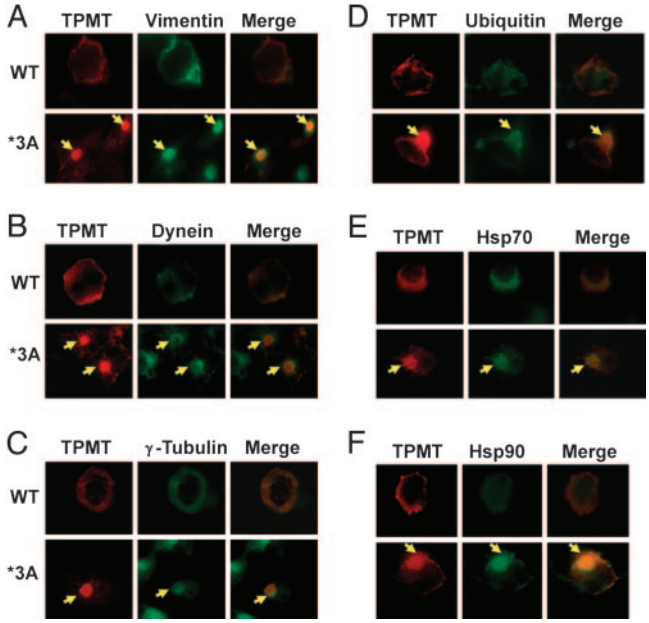

Fig. 3. Colocalization of TPMT*3A with aggresome components. COS-1 cells were transfected with WT or *3A HA-tagged TPMT constructs and were treated with MG132 before immunostaining with anti-HA polyclonal antibody (red) or monoclonal antibody directed against vimentin (*A*), dynein (*B*), γ-tubulin (*C*), Ub (*D*), hsp70 (*E*), or hsp90 (*F*) (green). Yellow arrows indicate aggresomes.

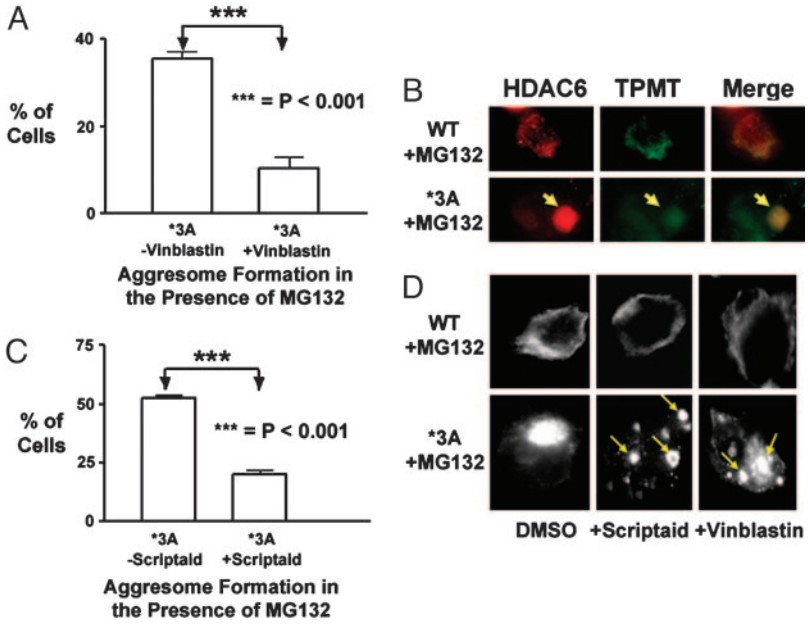

Fig. 4. Vinblastine and Scriptaid inhibited aggresome formation. (*A*) Cells transfected with HA-tagged TPMT*3A were treated with vinblastine and MG132 before staining with anti-HA antibody. Aggresome formation was expressed as a percentage of the total number of cells counted (mean ± SEM, $n = 4$). (*B*) TPMT*3A colocalization with HDAC6. Cells transfected with HA-tagged *3A were treated with MG132 and immunostained with monoclonal anti-HA antibody (green) and polyclonal anti-HDAC6 (red). (*C*) Scriptaid inhibited aggresome formation. In the presence of scriptaid, TPMT*3A aggresome formation also decreased significantly (mean ± SEM, $n = 4$, $P < 0.001$). (*D*) Both vinblastine and scriptaid failed to disrupt microaggregate formation (yellow arrows).

retrograde transport of misfolded proteins along microtubules, as demonstrated previously for other proteins (20, 26, 30).

HDAC6 also is essential for aggresome formation, presumably by serving as a connection between polyubiquitinated protein and dynein motors (31–34). TPMT*3A is polyubiquitinated (Fig. 2*B*) and thus is a candidate for HDAC6 linkage to dynein, so colocalization studies also were performed with polyclonal antibody to HDAC6. In the presence of MG132, HDAC6 colocalized to TPMT*3A-positive aggresomes (Fig. 4*B*). Furthermore, when cells were treated with the HDAC inhibitor scriptaid, aggresome number decreased significantly (Fig. 4*C*) (35). However, HDAC6 inhibition, like vinblastine treatment, failed to disrupt TPMT*3A microaggregate formation (Fig. 4*D*).

TPMT Allozyme Aggresome Formation, Degradation, and Chromatography. The facts that TPMT*3A is polyubiquitinated, is rapidly degraded, and forms aggresomes in the presence of MG132 support the hypothesis that the two SNPs shown in Fig. 1*A* might result in TPMT misfolding and aggregation. To explore the functional effects of those two SNPs further, we took advantage of the fact that the *TPMT*3A* allele has two SNPs, whereas the **3B* and**3C* alleles each have only one (Fig. 1*A*). Specifically, we compared aggresome formation, degradation in RRL, and behavior during size-exclusion chromatography for all three of these variant allozymes. The results for aggresome formation in COS-1 cells are shown in Fig. 5*A*, with a rank order of *3A > *3B > *3C > WT. Degradation was then performed with *in vitro*

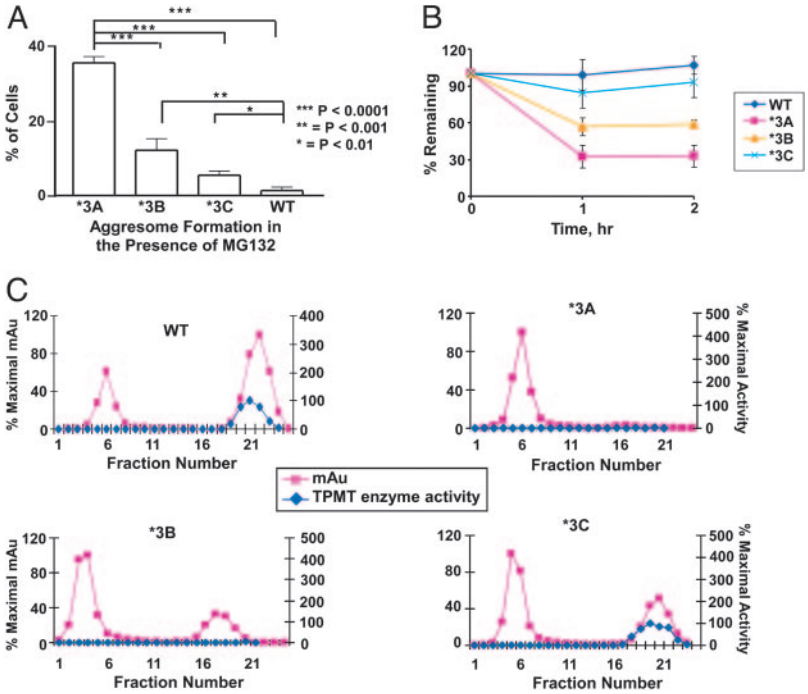

Fig. 5. TPMT allozyme aggresome formation, degradation, and size-exclusion chromatography. (*A*) Aggresome formation with WT, *3A, *3B, and *3C TPMT. Values are mean ± SEM ($n = 4$). (*B*) RRL degradation studies for TPMT allozymes. *In vitro* translated, radioactively labeled WT, *3A, *3B, and *3C TPMT were generated in RRL, followed by degradation studies. Values are mean ± SEM ($n = 3$). (*C*) Size-exclusion chromatography of purified bacterial recombinant WT, *3A, *3B, and *3C TPMT. The protein elution profile (percentage of peak milliabsorbance units, mAu) is shown in pink and TPMT enzyme activity in blue. Protein profiles are expressed as the percentage of peak mAu for protein concentrations, and TPMT enzyme activity is expressed as the percentage of peak enzyme activity. The initial peaks shown in *C* eluted with the void volumes, whereas second peaks eluted at ≈30 kDa. The first peak contained aggregated TPMT, whereas the second peak was TPMT monomers, based on SDS/PAGE and immunoblot analysis (data not shown).

translated [^{35}S]methionine-labeled TPMT proteins. We observed the same rank order for rates of protein degradation in RRL (Fig. 5*B*) as for aggresome formation, suggesting that these two SNPs might alter the structure of the protein, resulting in both accelerated degradation and aggregation.

To test directly whether the two SNPs present in *TPMT*3A* might predispose to protein aggregation, we next performed size-exclusion chromatography with *E. coli* recombinant TPMT. TPMT*3A eluted from the column close to the void volume, entirely as high molecular weight, presumably aggregated protein (Fig. 5*C*). *3B and *3C eluted 73% and 67% as aggregated protein, respectively; and 37% of the WT protein also was apparently aggregated, demonstrating that even the WT enzyme might have a tendency to aggregate. Size-exclusion chromatography was repeated a second time, with virtually identical results. Therefore, the data from size-exclusion chromatography correlated with the extent of aggresome formation in cultured cells and confirmed that both of the naturally occurring TPMT SNPs can promote protein aggregation. However, TPMT*3A eluted entirely as aggregated protein, suggesting that the simultaneous occurrence of these two alterations in encoded amino acid disrupted the TPMT structure, resulting in misfolding and aggregation. We also determined whether enzyme activity coeluted with monomers and/or aggregates. Activity eluted with WT and *3C monomers (Fig. 5*C*), but there was no activity in *3B monomers or any of the aggregates, suggesting that the codon 154 SNP might alter both the structure and the ability of the monomer to catalyze the enzyme reaction. Apparent K_m values of WT and *3C monomers for 6-mecaptopurine were 0.20 and 0.22 mM, respectively, whereas K_m values were 11 and 14 μM for the cosubstrate for the reaction, *S*-adenosyl-L-methionine (AdoMet). With 6-mecaptopurine as the varied substrate, V_{max} values were 107 and 94 nmol/h per μg of protein for WT and *3C monomers, respectively. When AdoMet was varied, V_{max} values were 120 and 90 nmol/h per μg of protein, respectively.

TPMT CD Spectroscopy. Potential structural differences among bacterially synthesized allozymes, purified by size-exclusion chromatography (Fig. 5*C*), also were studied by using CD spectroscopy. WT and *3C monomers had very similar spectra, with a trough at 224 nm, suggesting that WT and *3C may predominantly adopt β-sheet structure (Fig. 6*A*) (36). However, *3B had a lower signal and a shift of the peak to 220 nm, suggesting a significant change in secondary structure. This structural change also might be related to the lack of enzyme activity observed for *3B. The spectral peak for *3A aggregates also was significantly shifted, to 231 nm. CD thermal unfolding studies performed with WT, *3B and *3C monomers, and *3A aggregates showed that WT and *3C were able to unfold, following a two-state unfolding transition, but *3A did not show an unfolding transition, and *3B showed an apparent "transition" that was opposite in direction, with little signal change. We concluded that this change did not represent a true unfolding transition (Fig. 6*B*). Fraction folding curves (Fig. 6*C*) were used to calculate T_m values of 50°C and 39°C for WT and *3C monomers, respectively. Finally, in an attempt to study the structure of aggregates, EM was performed with equal amount of TPMT WT monomers and the *3A aggregates after chromatography. Before filtration, TPMT*3A formed dense amorphous aggregates. After filtration through a 2-μm filter, these aggregates were trapped and removed, whereas WT enzyme showed a smooth, even distribution of protein both before and after filtration (Fig. 7, which is published as supporting information on the PNAS web site).

Discussion

The results of our studies have demonstrated that the two common coding SNPs in TPMT result in structural disruption and misfolding of this clinically important drug-metabolizing enzyme, with protein aggregation and aggresome formation. Misfolded proteins can be removed from the cell by degradation, but they also can form aggregates (19, 21, 22). Aggresome formation represents a unique process by which cells can remove misfolded proteins (20). To test the possibility of aggresome formation for TPMT*3A, we first demonstrated that, in the presence of the proteasome inhibitor MG132, COS-1 cells transfected with TPMT*3A formed aggresomes (Fig. 1 *B* and *C*). That process correlated with the redistribution of TPMT protein from the soluble to insoluble portion of cell homogenates as demonstrated by immunoblot analysis (Fig. 2*A*). Previous studies in the RRL showed that TPMT*3A is targeted for degradation through a Ub-dependent, proteasome-mediated process. We next demonstrated that TPMT*3A was polyubiquitinated in COS-1 cells (Fig. 2*B*) as well as the RRL, and that polyubiquitinated TPMT*3A also was present in aggresomes (Fig. 2*C*). Aggresomes contain multiple molecular components. To determine the nature of TPMT*3A aggresomes, colocalization studies were performed that demonstrated that TPMT*3A aggresomes had the anticipated structure features (Fig. 3).

Aggresomes are formed from microaggregates of misfolded protein that are transported to the microtubule organizing

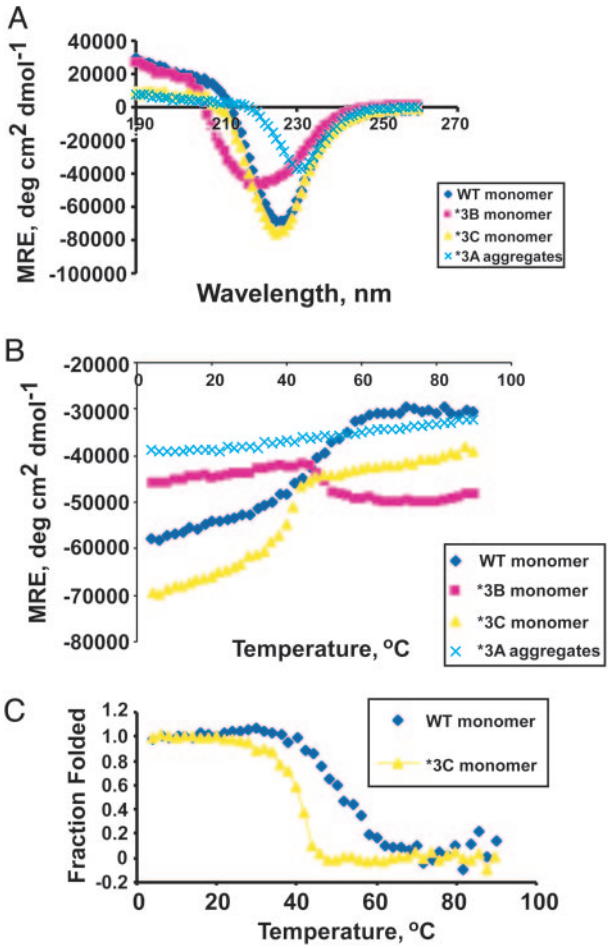

Fig. 6. Structural analysis of TPMT by using CD. (*A*) CD spectra for WT, *3B, and *3C TPMT monomers and for *3A aggregates. The WT (blue line) and *3C (yellow line) monomers had very similar spectra, with mean residue ellipticity (MRE) signals of approximately $-8{,}000$ deg·cm^2·dmol^{-1} at 224 nm, whereas the MRE value for the *3B monomer (pink line) was $-5{,}000$ deg·cm^2·dmol^{-1} at 220 nm. (*B*) CD thermal unfolding studies. (*C*) TPMT WT and *3C monomer folding curves derived from the data shown in *B*.

center, with the involvement of the microtubule network and the retrograde motor protein, dynein (20, 25, 26). In the presence of the microtubule destabilizing agent vinblastine, TPMT*3A aggresome formation was disrupted (Fig. 4*A*). However, this drug, as anticipated, failed to disrupt microaggregates (Fig. 4*D*). The HDACs are a family of enzymes whose functions have been associated most often with chromatin dynamics and with the regulation of gene expression (37). However, recent evidence indicates that HDACs have functions that extend beyond the regulation of gene transcription and chromatin remodeling (38). For example, HDAC6 shows extensive colocalization with $p150^{glued}$ (33), a component of the dynein motor complex. HDAC6 contains a Ub-binding zinc finger and is associated with ubiquitinated proteins after proteasome inhibition (32, 39). Kawaguchi *et al.* (34) recently demonstrated that HDAC6 can link misfolded polyubiquitinated proteins to the dynein microtubule network. Therefore, it seemed reasonable to test the possible involvement of HDAC6 in TPMT*3A aggresome formation. The fact that HDAC6 colocalized with *3A in the aggresome (Fig. 4*B*) and that the specific HDAC inhibitor scriptaid reduced aggresome formation (Fig. 4*C*) suggests that HDAC6 might connect polyubiquitinated TPMT*3A with the dynein motor complex, thus facilitating the transport of TPMT*3A to the aggresome. The fact that scriptaid inhibited aggresome, but not microaggregate, formation (Fig. 4*D*), also was compatible with this conclusion.

*TPMT*3A* contains two common polymorphisms, whereas the *3B and *3C alleles each have only one of these two polymorphisms (Fig. 1*A*). To study the impact of these two SNPs individually, we compared the variant TPMT allozymes *3A, *3B, and *3C with regard to aggresome formation, the rate of allozyme degradation in the RRL, and their structural properties, as determined by size-exclusion chromatography and CD spectroscopy. The half-lives of these allozymes in the RRL had a similar rank order with that for aggresome formation (Fig. 5 *A* and *B*). *E. coli* recombinant protein for all four allozymes was used to directly test their tendency to aggregate by performing size-exclusion chromatography. The results indicated that even the WT protein has a tendency to aggregate, which might help to explain why it has proven difficult to crystallize TPMT (40). The proportions of aggregated protein eluting from the FPLC size-exclusion column also were consistent with the results for aggresome formation in COS-1 cells and the rates of RRL degradation for WT and the three variant allozymes (Fig. 5). The WT and *3C monomers had comparable K_m values for the two cosubstrates for the reaction, but the *3B monomer had virtually no activity. The fact that *3B is misfolded, plus the fact that its monomer has no activity (Fig. 5*C*), may explain why there is no detectable activity when this allozyme is expressed in cultured cells.[¶] These results provide evidence that the proteins encoded by TPMT alleles with these two SNPs, either alone, or, even more striking, together, are misfolded. Furthermore, the exon 7 SNP, G460A, which is present in both TPMT*3A and TPMT*3B also might affect the catalytic ability of the protein (Fig. 5*C*).

Taken together, these results indicate that TPMT*3A is misfolded and, therefore, aggregates and is targeted for degradation. The very low level of TPMT*3A protein in human tissues is probably due to both aggregation and the rapid degradation of TPMT monomers and aggregates, with these processes existing in dynamic balance. In summary, we have demonstrated that the the *TPMT*3A* SNPs disrupt the structure of the enzyme, resulting in misfolding, aggregation, and, ultimately, in life-threatening thiopurine toxicity in patients treated with standard doses of these drugs. These observations also might have mechanistic implications for other pharmacogenetically important polymorphisms.

[¶]Salavaggione, O. E., Wiepert, M. & Weinshilboum, R. M. (2004) *Clin. Pharmacol. Ther.* **75,** P19 (abstr.).

This work was partially supported by National Institutes of Health Grants R01GM28157 (to L.W., T.V.N., and R.M.W.), R01GM35720 (to L.W. and R.M.W.), and U01GM61388, the Pharmacogenetics Research Network (L.W. and R.M.W.), the Mayo Foundation (M.R.-A. and L.A.S.), and the Mayo Foundation Hematology Malignancies Program (R.W.M.).

1. Weinshilboum, R. & Wang, L. (2004) *Nat. Rev. Drug Discov.* **3,** 739–748.
2. Remy, C. N. (1963) *J. Biol. Chem.* **238,** 1078–1084.
3. Woodson, L. C. & Weinshilboum, R. M. (1983) *Biochem. Pharmacol.* **32,** 819–826.
4. Lennard, L., Van Loon, J. A. & Weinshilboum, R. M. (1989) *Clin. Pharmacol. Ther.* **46,** 149–154.
5. Lennard, L. (1992) *Eur. J. Clin. Pharmacol.* **43,** 329–339.
6. Evans, W. E., Horner, M., Chu, Y. Q., Kalwinsky, D. & Roberts, W. M. (1991) *J. Pediatr.* **119,** 985–989.
7. Weinshilboum, R. M. & Sladek, S. L. (1980) *Am. J. Hum. Genet.* **32,** 651–662.
8. Woodson, L. C., Dunnette, J. H. & Weinshilboum, R. M. (1982) *J. Pharmacol. Exp. Ther.* **222,** 174–181.
9. Szumlanski, C. L., Honchel, R., Scott, M. C. & Weinshilboum, R. M. (1992) *Pharmacogenetics* **2,** 148–159.
10. Szumlanski, C., Otterness, D., Her, C., Lee, D., Brandriff, B., Kelsell, D., Spurr, N., Lennard, L., Wieben, E. & Weinshilboum, R. (1996) *DNA Cell Biol.* **15,** 17–30.
11. Weinshilboum, R. M., Otterness, D. M. & Szumlanski, C. L. (1999) *Ann. Rev. Pharmacol. Toxicol.* **39,** 19–52.
12. Weinshilboum, R. (2003) *N. Engl. J. Med.* **348,** 529–537.
13. Schütz, E., Gummert, J., Mohr, F. & Oellerich, M. (1993) *Lancet* **341,** 436.
14. Weinshilboum, R. (2001) *Drug Metab. Dispos.* **29,** 601–605.
15. Department of Health and Human Services Food and Drug Administration, Center for Drug Evaluation and Research, Center for Biologics Evaluation and Research, and Center for Devices and Radiological Health (November 2003) *Draft Guidance for Pharmacogenomic Data Submission*.
16. Wang, L., Sullivan, W., Toft, D. & Weinshilboum, R. (2003) *Pharmacogenetics* **13,** 555–564.
17. Tai, H.-L., Fessing, M. Y., Bonten, E. J., Yanishevsky, Y., d'Azzo, A., Krynetski, E. Y. & Evans, W. E. (1999) *Pharmacogenetics* **9,** 641–650.
18. Weinshilboum, R. & Wang, L. (2004) *Clin. Pharmacol. Ther.* **75,** 253–258.
19. Wickner, S., Maurizi, M. R. & Gottesman, S. (1999) *Science* **286,** 1888–1893.
20. Johnston, J. A., Ward, C. L. & Kopito, R. R. (1998) *J. Biol. Chem.* **143,** 1883–1898.
21. Kopito, R. R. (2000) *Trends Cell Biol.* **10,** 524–530.
22. Garcia-Mata, R., Gao, Y. S. & Sztul, E. (2002) *Traffic* **3,** 388–396.
23. Barent, R. L., Nair, S. C., Carr, D. C., Ruan, Y., Rimerman, R. A., Fulton, J., Zhang, Y. & Smith, D. F. (1998) *Mol. Endocrinol.* **12,** 342–354.
24. Weinshilboum, R. M., Raymond, F. A. & Pazmiño, P. A. (1978) *Clin. Chim. Acta.* **85,** 323–333.
25. Wigley, W. C., Fabunmi, R. P., Lee, M. G., Marino, C. R., Muallem, S., DeMartino, G. N. & Thomas, P. J. (1999) *J. Cell Biol.* **145,** 481–490.
26. Garcia-Mata, R., Bebok, Z., Sorscher, E. J. & Sztul, E. S. (1999) *J. Cell. Biol.* **146,** 1239–1254.
27. Dictenberg, J. B., Zimmerman, W., Sparks, C. A., Young, A., Vidair, C., Zheng, Y., Carrington, W., Fay, F. S. & Doxsey, S. J. (1998) *J. Cell Biol.* **141,** 163–174.
28. Hartl, F. U. & Martin, J. (1995) *Curr. Opin. Struct. Biol.* **5,** 92–102.
29. Wojcik, C., Schroeter, D., Wilk, S., Lamprecht, J. & Paweletz, N. (1996) *Eur. J. Cell. Biol.* **71,** 311–318.
30. Johnston, J. A., Dalton, M. J., Gurney, M. E. & Kopito, R. R. (2000) *Proc. Natl. Acad. Sci. USA* **97,** 12571–12576.
31. Zhang, Y., Li, N., Caron, C., Matthias, G., Hess, D., Khochbin, S. & Matthias, P. (2003) *EMBO J.* **22,** 1168–1179.
32. Hook, S. S., Orian, A., Cowley, S. M. & Eisenman, R. N. (2002) *Proc. Natl. Acad. Sci. USA* **99,** 13425–13430.
33. Hubbert, C., Guardiola, A., Shao, R., Kawaguchi, Y., Ito, A., Nixon, A., Yoshida, M., Wang, X. F. & Yao, T. P. (2002) *Nature* **417,** 455–458.
34. Kawaguchi, Y., Kovacs, J. J., McLaurin, A., Vance, J. M., Ito, A. & Yao, T. P. (2003) *Cell* **115,** 727–738.
35. Corcoran, L. J., Mitchison, T. J. & Liu, Q. (2004) *Curr. Biol.* **14,** 488–492.
36. Venyaminov, S. Y. & Vassilenko, K. S. (1996) *Anal. Biochem.* **222,** 176–184.
37. Ayer, D. E. (1999) *Trends Cell Biol.* **9,** 193–198.
38. Verdin, E., Dequiedt, F. & Kasler, H. G. (2003) *Trends Genet.* **19,** 286–293.
39. Seigneurin-Berny, D., Verdel, A., Curtet, S., Lemercier, C., Garin, J., Rousseaux, S. & Khochbin, S. (2001) *Mol. Cell. Biol.* **21,** 8035–8044.
40. Scheuermann, T. H., Lolis, E. & Hodsdon, M. E. (2003) *J. Mol. Biol.* **333,** 573–585.
41. Wang, L., Yee, V. C. & Weinshilboum, R. M. (2004) *Biochem. Biophys. Res. Commun.* **325,** 426–433.